Uncertainties in Biologically-Based Modeling of Formaldehyde-Induced Respiratory Cancer Risk: Identification of Key Issues

Ravi P. Subramaniam,[1]* Chao Chen,[1] Kenny S. Crump,[2] Danielle DeVoney,[1] John F. Fox,[1] Christopher J. Portier,[3] Paul M. Schlosser,[1] Chad M. Thompson,[1] and Paul White[1]

In a series of articles and a health-risk assessment report, scientists at the CIIT Hamner Institutes developed a model (CIIT model) for estimating respiratory cancer risk due to inhaled formaldehyde within a conceptual framework incorporating extensive mechanistic information and advanced computational methods at the toxicokinetic and toxicodynamic levels. Several regulatory bodies have utilized predictions from this model; on the other hand, upon detailed evaluation the California EPA has decided against doing so. In this article, we study the CIIT model to identify key biological and statistical uncertainties that need careful evaluation if such two-stage clonal expansion models are to be used for extrapolation of cancer risk from animal bioassays to human exposure. Broadly, these issues pertain to the use and interpretation of experimental labeling index and tumor data, the evaluation and biological interpretation of estimated parameters, and uncertainties in model specification, in particular that of initiated cells. We also identify key uncertainties in the scale-up of the CIIT model to humans, focusing on assumptions underlying model parameters for cell replication rates and formaldehyde-induced mutation. We discuss uncertainties in identifying parameter values in the model used to estimate and extrapolate DNA protein cross-link levels. The authors of the CIIT modeling endeavor characterized their human risk estimates as "conservative in the face of modeling uncertainties." The uncertainties discussed in this article indicate that such a claim is premature.

KEY WORDS: Biologically-based dose response; formaldehyde; two-stage cancer model

1. INTRODUCTION

Biologically-based models have the potential to reduce scientific uncertainties in risk assessment by replacing default methods with appropriate data. These models often require various assumptions in the selection of model structure and identification of key parameters that influence model predictions. Even where data are available to inform a parameter or model component, normal variability and measurement errors exist. Depending on model uncertainties and the sensitivity of model predictions to these uncertainties, one can develop a hierarchy of biologically-based dose-response (BBDR) models whose utility can range from generating scientifically significant hypotheses and the analysis of experimental and epidemiologic data to predicting risks from human exposures. Determining the

[1] NCEA, ORD, U.S. Environmental Protection Agency, Pennsylvania Ave. NW, Washington, DC, USA .
[2] Louisiana Tech University, Ruston, LA, USA.
[3] NIEHS, National Institutes of Health, Research Triangle Park, NC, USA.
* Address correspondence to Ravi P. Subramaniam, NCEA, ORD, U.S. Environmental Protection Agency, Mailcode 8623-P, 1200 Pennsylvania Ave. NW, Washington, DC 20460, USA; tel: (703)-347-8606; fax: (703) 347-8694; Subramaniam.Ravi@epa.gov.
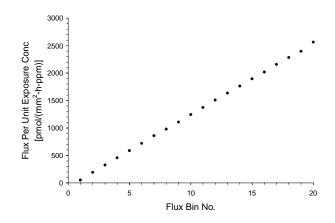
placement of a model within this hierarchy is crucial. Recently, scientists at the CIIT Hamner Institutes developed a mathematical model to predict respiratory cancer risk at environmental exposures due to inhaled formaldehyde with emphasis on using available mechanistic information and using multiple computational models to interpret bioassay data (CIIT, 1999; Conolly *et al.*, 2000, 2003, 2004; Kimbell *et al.*, 2001a, 2001b; Overton *et al.,* 2001). We refer to these efforts collectively as the CIIT model. The purpose of this article is two-fold:

1. to identify issues that need careful evaluation when BBDR models such as the CIIT formaldehyde model are used for risk extrapolation purposes and
2. to identify various biological inferences and hypotheses that can be generated using this model, but that have not been indicated in previous publications related to the CIIT model, and to discuss their plausibility in the context of the biological information at hand.
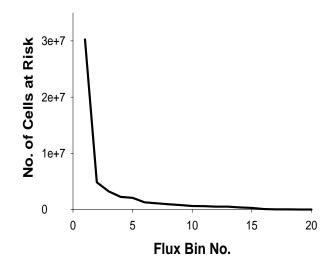
The CIIT risk assessment utilized data from two long-term bioassays that found increased incidence of nasal squamous cell carcinomas (SCC) in rats exposed to formaldehyde by inhalation (Kerns *et al.*, 1983; Monticello *et al.*, 1996). The resulting tumor occurrence was modeled using an approximation of the two-stage clonal growth model (Moolgavkar *et al.*, 1988) and allowing formaldehyde to have directly mutagenic action. The model was initially calibrated to the tumor data in rats (Conolly *et al.*, 2003) and subsequently extended to predict tumor risk in humans (Conolly *et al.*, 2004). The inputs to the two-stage modeling consisted of:

1. Regional uptake of formaldehyde in the respiratory tract predicted using computational fluid dynamics (CFD) modeling in the F344 rat and humans (Kimbell *et al.*, 2001a, 2001b; Overton *et al.*, 2001; Subramaniam *et al.*, 1998);
2. Concentrations of DNA protein cross-links (DPX) in F344 rats and rhesus monkeys predicted by a physiologically-based pharmacokinetic (PBPK) model (Conolly *et al.*, 2000); and
3. Cell division rates inferred from labeling index data on rats exposed to formaldehyde (Monticello *et al.*, 1990, 1991, 1996).

A novel contribution of the CIIT model is that cell division rates and DPX concentrations are driven

Fig. 1. Flux bins in the model for formaldehyde dosimetry in the F344 rat nose. Y-axis is average formaldehyde flux per ppm of exposure concentration in a given flux bin. In the model, flux scales linearly with exposure concentration (ppm).

Fig. 2. Distribution of cells at risk across flux bins in the F344 rat nasal lining.

by the local concentration of formaldehyde. This was achieved by partitioning the nasal surface by formaldehyde flux to the tissue, resulting in 20 "flux bins" (Fig. 1). Each bin comprises elements (not necessarily contiguous) of the nasal surface that receive a particular interval of formaldehyde flux per ppm of exposure concentration (Kimbell *et al.*, 2001a). The spatial coordinates of elements comprising a particular flux bin are fixed for all exposure concentrations, with formaldehyde flux in a bin scaling linearly with exposure concentration (ppm). The number of cells at risk varies across the bins, as shown in Fig. 2.

The modeling effort in Conolly *et al.* (2003) inferred that the tumorigenicity of formaldehyde in Fisher's 344 (F344) rats could be optimally (in the statistical sense) explained on the basis of cytotoxicity-driven regenerative cell proliferation, without *any* contribution from a direct formaldehyde-induced mutagenic component. Extrapolation of the cancer risk to humans with a scale-up of this model produces a *deminimis* added risk due to mutagenicity at environmental exposure levels using a statistical upper bound on the estimated parameter associated with this mutagenic component (Conolly *et al.*, 2004). Predictions from the CIIT model have been utilized by several regulatory bodies in either deriving or as further evidence supporting exposure standards for formaldehyde (BfR, 2006; Health Canada, 2001; Liteplo & Meek, 2003; MAK Commission, 2006; USEPA, 2006a, 2006b). On the other hand, the California Environmental Protection Agency decided against using the CIIT modeling effort, citing the need for examining model uncertainty (CalEPA, 2005).

In a previous article (Subramaniam *et al.*, 2007), we quantitatively examined the following uncertainties in Conolly *et al.* (2003): (a) the impact of applying solutions to the two-stage model that are valid only for a time-independent model, (b) the assumption of rapidly fatal tumors, and (c) the impact of including historical controls from all National Toxicology Program (NTP) bioassays. In contrast to the conclusion in Conolly *et al.* (2003, 2004), we showed that, depending on the control data used, a large contribution from formaldehyde's mutagenic action may be needed in the mathematical model to explain formaldehyde carcinogenicity. The focus of this article is to outline additional uncertainties in Conolly *et al.* (2003, 2004) and the inferences that can be drawn from their modeling. These issues pertain to

1. the characterization of normal cell replication rates,
2. the model structure for relating initiated cell division and death rates to corresponding rates in normal cells,
3. the extrapolation of cell replication rates to humans from those characterized for the F344 rat, and
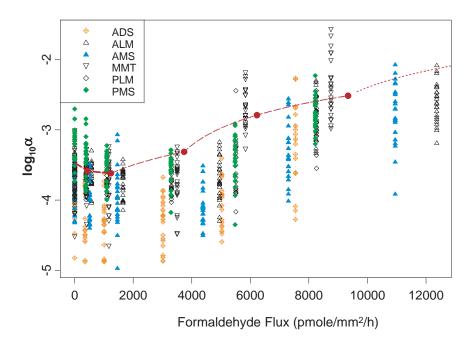4. the use and extrapolation of data on DNA protein cross-links.

2. KEY ISSUES AND INFERENCES

2.1. Replication Rates for Normal Cells (α_N)

Cell replication rates in Conolly *et al.* (2003) were obtained by pooling labeling data from two phases of a study in which male F344 rats were exposed to formaldehyde gas at similar concentrations (0., 0.7, 2.0, 6.0, 10.0, or 15.0 ppm). The first phase employed injection labeling with a two-hour pulse labeling time and animals were exposed to formaldehyde for early exposure periods of 1, 4, and 9 days, and 6 weeks (Monticello *et al.*, 1991). The second phase used osmotic minipumps for labeling with a 120-hour labeling time to quantify labeling in animals exposed for 13, 26, 52, and 78 weeks (Monticello *et al.*, 1996). Considerable uncertainty and variability, both quantitative and qualitative, exist in the use and interpretation of these labeling data for characterizing a dose response for cell replication rates. We discuss the primary issues here.

Monticello *et al.* (1991, 1996) used unit length labeling index (ULLI) to quantify cell replication within the respiratory epithelium. ULLI is a ratio between a count of labeled cells and the corresponding length (in millimeters) of basal membrane examined, whereas the per-cell labeling index (LI) is the ratio of labeled cells to all epithelial cells, in this case, along some length of basal membrane and its associated layer of epithelial cells. Monticello *et al.* (1991, 1996) published ULLI values averaged over replicate animals for each combination of exposure concentration, exposure time, and nasal site. Conolly *et al.* (2003) adopted the following procedure to construct a dose-response curve for normal cell replication rates (α_N as a function of formaldehyde flux) from these data.

1. The injection labeled ULLI data were first normalized by the ratio of the average minipump ULLI for controls to the average injection labeled ULLI for controls.
2. The ULLI average values (after the above normalization) were then weighted by the exposure times in Monticello *et al.* (1991, 1996) and averaged over the nasal sites. Thus, the data were combined into one time-weighted average for each exposure concentration.
3. LI was linearly related to the measured ULLI using data from a different experiment (Monticello *et al.*, 1990) where both quantities had been measured for two sites in the nose. The
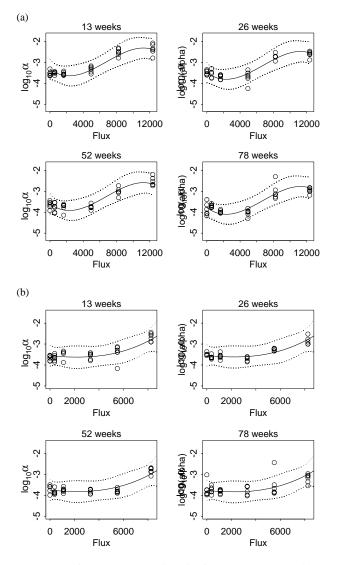
Fig. 3. Logarithm of normal cell replication rate α_N versus formaldehyde flux (in units of pmol/mm^2/h) for the F344 rat nasal epithelium. Values were derived from continuous unit length labeled data obtained by Monticello *et al.* (1996), for 4–6 individual animals at all 6 nasal sites (legend, sites as denoted in original article) and 4 exposure durations (13, 26, 52, 78 weeks). Each point represents a measurement for one rat, at one nasal site, and at a given exposure time. Filled red circles: α_N(flux) used in Conolly *et al.* (2003) plotted at their averaged flux values (see text for details). Long dashed lines: their linear interpolation between points. Short dashed line: their linear extrapolation for flux value >9,340 pmol/mm^2/h (see Fig. 5 for full range of extrapolation). *Note*: Linear interpolation/extrapolation is shown with y-axis transformed to logarithmic scale.

mean value of 0.60 for the ratio ULLI/LI was then used.

4. Cell replication rates of normal cells (α_N) were then calculated using an approximation due to Moolgavkar and Luebeck (1992); given by $\alpha_N = (-0.5/t)\log(1 - \text{LI})$, where LI is the labeling index, and t is the period of labeling (120 hours; Monticello *et al.*, 1996).

5. This was repeated for each exposure concentration of formaldehyde, resulting in one value of α_N for each exposure concentration.

6. Correspondingly, for a given exposure concentration, the steady-state formaldehyde flux into tissue, computed by CFD modeling, was averaged over all nasal sites. Thus, the α_N(flux) constructed by Conolly *et al.* (2003) consisted of a single α_N and a single average flux for each of six exposures.

However, the formula for α_N in Step 4 above was derived for continuous labeled index, and Moolgavkar and Luebeck caution that it is not applicable for pulse-labeled data. The application of this formula to the injection (pulse)-labeled data is problem-

atic because two-hour pulse-labeled data represent the pool of cells in S-phase rather than the rate at which cells are recruited to the pool and because the baseline values of α_N obtained in this manner from both data sets differ considerably. Therefore, we restrict our analysis below to the continuous labeled data (Monticello *et al.*, 1996).

Fig. 3 shows the variability due to replicate animals, exposure times, and nasal sites in the continuous labeled data obtained by Monticello *et al.* (1996). The unit length labeling index data for individual animals were provided to us by CIIT. In this figure, we plotted log α_N versus site-specific flux for six sites and four exposure times for four to six replicate animals in each case. Each point represents data from a single site for a single animal at a given time. The α_N(flux) tabulated in Conolly *et al.* (2003) are also plotted in this figure at their averaged flux values (filled circles). For flux >9,340 pmol/mm^2/h, Conolly *et al.* extrapolated this empirically derived α_N(flux) using a scheme discussed below in Section 2.1.1. The curves shown connecting the filled circles in the figure represent their linear interpolation (long dashes) between the six points. Their linear

(a)

(b)

Fig. 4. Logarithm of normal cell replication rate versus formaldehyde flux with simultaneous confidence limits for two of the largest sites in the F344 rat nose: (a) for the anterior lateral meatus (ALM); (b) for the posterior lateral meatus (PLM).

extrapolation for flux value >9,340 pmol/mm^2/h is also shown (short dashes). Note that the linear interpolation/extrapolation is shown transformed to a logarithmic scale here.

In Figs. 4(a), and 4(b), we plot our fitted dose-response curves for $\log_{10}(\alpha_N)$ versus flux with simultaneous confidence limits separately for each time point for two of the largest sites in the rat nose (anterior lateral meatus, ALM, and posterior lateral meatus, PLM). Note that flux levels are different at each site. We used simple polynomial models in flux (as a continuous predictor), with time included as a factor

(i.e., a class or indicator variable, τ_i representing the effect of the ith time),

$$\log(\alpha_N) = a + b \cdot \text{flux} + c \cdot \text{flux}^2 + d \cdot \text{flux}^3 + \tau_i.$$
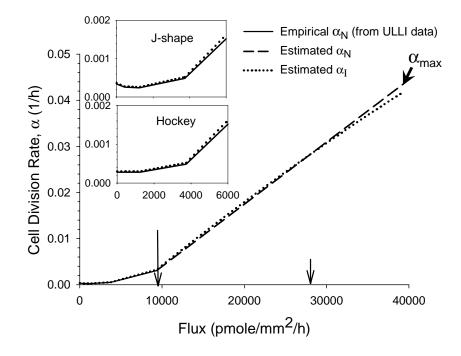
The variability considered is that among animals and any measurement error as well as any other design-related components of error. Simultaneous 95% confidence limits for $\log(\alpha_N)$ were produced using Scheffe's method (Snedecor & Cochran, 1980). These 95% confidence limits span a range of 0.96 in $\log_{10}(\alpha_N)$, or nearly a 10-fold range in median α_N. There is additional dispersion in these data that does not appear in Figs. 3 and 4(a), 4(b); due to variation in the number of cells per mm basement membrane, the ratio of ULLI/LI had a spread of approximately ±25% (0.45 to 0.71, mean 0.60) among the eight observations considered in Monticello *et al.* (1990).

Conolly *et al.* (2003) obtained a "J-shaped" dose-response curve for cell replication (when viewed on a nontransformed scale for α_N), as also shown in Fig. 5 for the full range of flux values used in their modeling. They also considered a hockey-stick-threshold representation of their J-shaped curve for α_N in order to make a health-protective choice, and the differences between the two can be seen from the insets in Fig. 5. In these curves, the cell replication rate is less than or the same as the baseline cell replication rate at low formaldehyde flux values. Gaylor *et al.* (2004) also analyzed the time-weighted averages of the combined ULLI data and found the dose-response curves so derived to be J-shaped at various sites. The shape of the dose-response curve for cell replication as characterized in Conolly *et al.* (2003) is seen as representing regenerative cell proliferation secondary to the cytotoxicity of formaldehyde (Conolly *et al.*, 2002). By extending the shape of these curves to initiated cells, the model brings the cytotoxic action of formaldehyde to bear strongly upon the parameterization of the model for the F344 rat as well as the humans.

The six nasal sites represented both high and low flux regions and also differed significantly in the population of dividing cells at these sites, and varied by roughly an order of magnitude in the labeling index (Monticello *et al.*, 1996; Kimbell *et al.*, 2001b). As suggested by Figs. 4(a), and 4(b), the shape of α_N(flux) in Conolly *et al.* (2003) is therefore sensitive to the specific averaging scheme used by these authors. Averaging of sites could significantly affect model calibration because of substantial nonlinearity in model dependence on α_N at the 10 ppm and 15 ppm doses

Fig. 5. Dose response of normal (α_N) and initiated (α_I) cell division rate in Conolly *et al.* (2003). Empirically derived values of α_N (time-weighted average over six sites) from Table 1 in Conolly *et al.* (2003) and optimized parameter values from their Table 4 were used. Main panel is for the "J-shape" dose response. Insets show "J-shape" and "hockey-stick" representations at low end of flux range. Long arrow denotes upper end of flux range for which the empirical unit-length labeling data are available for use in the clonal growth model. α_{max} is value of α_N at the maximum formaldehyde flux delivered at 15 ppm exposure, and estimated by optimizing against the tumor incidence data. $\alpha_I < \alpha_N$ for flux greater than value indicated by small vertical arrow. Conolly *et al.* (2003, 2004) assumed $\beta_I = \alpha_N$ at all flux values.

associated with high cancer incidence. Monticello *et al.* found a high correlation between tumor rate and the unit length labeling index weighted by the number of cells at a site. Therefore, considering these factors while regressing α_N against tissue dose would be important in the context of site differences in tumor response. A further complexity arises because of histological changes and thickening that occurs in the nasal epithelium over time in the higher-dose groups (Morgan, 1997), factors that are likely to affect estimates of replication rates.

The more relevant question, however, is whether the use of a time-weighted average over all sites has an effect on low-dose risk estimates. It would also be useful to examine if the time-dependence affects the results of the time-to-tumor modeling and whether early temporal changes in replication rate are important to consider because of the generally cumulative nature of cancer risk. The time window over which formaldehyde-induced cancer risk is most influenced is not known, but the time weighting assigns a relatively low weight to labeling observed at early times compared with those observed at later time points. Finally, initiated cells are likely to be replicating at higher rates than normal cells as evidenced in several studies on premalignant lesions (Rotstein *et al.,* 1986; Dragan *et al.*, 1995; Coste *et al.*, 1996). Therefore, labeling index data as an estimator of normal cell replication rate would be most reliable at early times when the mix of cell samples in-

cludes fewer preneoplastic or neoplastic cells. Given the above uncertainties and variability not characterized in CIIT (1999) or in Conolly *et al.* (2003), we believe it is important to examine whether additional dose-response curves that fit the cell replication data reasonably well have an impact on estimated risk.

2.1.1. Upward Extrapolation of Normal Cell Division Rate

The extensive labeling data collected by Monticello *et al.* (1991, 1996) present an opportunity to use precursor data in assessing cancer risk. The attempt to apply these data (collected at specific sites and as averaged) to the full set of 20 flux bins from the CFD model, however, leads to a difficulty in Conolly *et al.* (2003). Because of the averaging and the fact that replication data were not collected at sites where the very highest fluxes are predicted to occur, the empirical data could only be used to determine $\alpha_N(\text{flux})$ for the lower flux range, 0–9, 340 pmol/mm²/h, whereas the highest computed flux at 15.0 ppm exposure was 39,300 pmol/mm²/h. Therefore, Conolly *et al.* introduced an adjustable parameter, α_{max}, that represented the value of $\alpha_N(\text{flux})$ at the maximum flux of 39,300 pmol/mm²/h. α_{max} was estimated by maximizing the likelihood of the two-stage model fit to the tumor incidence data. For $9{,}340 < \text{flux} \le 39{,}300$ pmol/mm²/h, $\alpha_N(\text{flux})$ was determined

by linear interpolation from $\alpha_N(9,340)$ to α_{max}, as shown by the dashed line in Fig. 5.

2.2. Division and Death Rate of Initiated Cells

The results of a two-stage model are extremely sensitive to the values for initiated cell division (α_I) and death (β_I) rates, particularly in the case of a sharply rising dose-response curve as in the case of formaldehyde. The pool of cells used for obtaining the available labeling index data (Monticello *et al.*, 1991, 1996) consists of largely normal cells with perhaps increasing numbers of initiated cells at higher exposure concentrations. Since the division rates of initiated cells in the nasal epithelium, either background or formaldehyde-exposed, could not be inferred from the available empirical data, Conolly *et al.* made what they perceived to be a biologically reasonable assumption for α_I. Conolly *et al.* assumed α_I to be linked to α_N by

$$\alpha_I = \alpha_N\{multb - multc \times \max[\alpha_N - \alpha_{N(basal)}, 0]\}, \tag{1}$$

where $\alpha_N \equiv \alpha_N(\text{flux})$, $\alpha_{N(basal)}$ is the estimated average cell division rate in unexposed normal cells, and *multb* and *multc* are unknown parameters estimated by likelihood optimization against the tumor data.[4] Dose-response curves for α_N and α_I in the Conolly *et al.* model are depicted in Fig. 5. The main panel in this figure was generated using the J-shaped cell replication dose response and the optimized values of the parameters in Conolly *et al.* (2003) for this case.

As shown in Fig. 5, α_I is estimated in Conolly *et al.* (2003) to be very similar to α_N. That is, with Equation (1) assumed to relate $\alpha_I(\text{flux})$ to $\alpha_N(\text{flux})$, a J (or hockey)-shaped dose-response curve for $\alpha_N(\text{flux})$ results in a J (or hockey) for $\alpha_I(\text{flux})$. The J-shape for the time-weighted averaged $\alpha_N(\text{flux})$ in Conolly *et al.* (2003) could plausibly be explained, as suggested by the examples in Conolly and Lutz (2004), by a mathematical superposition of dose-response curves describing the effects of (a) the inhibition of cell replication by the formation of DPX (Heck & Casanova, 1999), and (b) cytotoxicity-induced regenerative replication (Conolly *et al.*, 2002). As explained earlier, there is considerable uncertainty and variability, both qualitative and quantitative, in the interpretation of the labeling index data, and in the derivation of cell replication rates from the unit-length labeling index data. Notwithstanding this uncertainty-variability, and in the absence of data, the essential question is whether mechanisms that explain a J-shaped dose response for normal cell replication or a cytotoxicity-driven threshold in doseresponse (as indicated by a hockey-stick-shaped curve) should be expected to prevail also for initiated cells. Furthermore, would the formaldehyde flux at which the cell replication dose-response curve rises above its baseline be similar in value for both normal and initiated cells as inferred by the CIIT model in Fig. 5?

In general, normal and initiated cells represent distinctly different cell populations with regard to proliferation response (Ceder *et al.,* 2007; Dragan *et al.*, 1995; Coste *et al.*, 1996; Schulte-Hermann *et al.*, 1997; Bull, 2000). The hypothesis that formaldehyde-induced DPX blocks cell replication, a step that requires activation of a checkpoint in the cell cycle for DNA repair, was made for normal cells. If exposure to formaldehyde leads to loss of function of p53 or other key cell cycle genes in the rat via mutation, deletion, or silencing, then it is less likely that DNA replication would be blocked in such cells. p53 mutations have been identified in formaldehyde-induced preneoplastic and neoplastic lesions in nasal passages of rats exposed to 15 ppm formaldehyde[5] (Recio *et al.*, 1992, 1997; Wolf *et al.*, 1995); these data are discussed further below. Furthermore, initiated cells are generally thought to be resistant to the cytotoxicity that inhibits proliferation in a normal cell (Farber, 1984; Tsuda *et al.*, 1980; Glick & Yuspa, 1994).

The hazard function in Conolly *et al.* (2003) depends on the birth rate (α_I) and death rates (β_I) of initiated cells (as opposed to depending only on the net rate, $\alpha_I - \beta_I$). The calibration of the model in Conolly *et al.* (2003) is most influenced by the high-dose animal data while its use in Conolly *et al.* (2004) is for low-dose human exposure. Parameters α_I and β_I are therefore separately important to this problem in contrast to some epidemiologic applications where only the difference is critical (Moolgavkar & Luebeck, 1990). In the absence of data, it is therefore necessary to make a reasonable assumption regarding β_I in order to implement a two-stage model. Conolly *et al.* (2003, 2004) considered β_I to be a

---

[4]*multb* and *multc* were equal to 1.072 and 2.583, respectively (J-shaped α_N), and 1.070 and 2.515, respectively (hockey-stick shaped α_N).

[5]It may be noted that p53 mutations have also been indicated by the data of Shaham *et al.* (2003) in human exposures to formaldehyde well below cytotoxic concentrations, although the reliability of these data has been questioned.
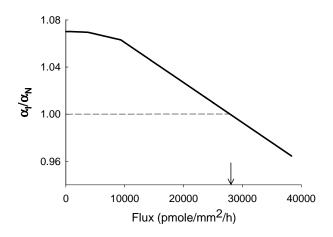
function of local formaldehyde flux, and related this parameter to the cell division rate of normal cells. They assumed

$$\beta_{\text{I}}(\text{flux}) = \alpha_N(\text{flux}). \quad (2)$$

(Note that the growth of the population of normal cells is specified in a deterministic manner, so the death rate of *normal* cells β_N does not explicitly enter the dynamics.)

In the rest of this section, we seek plausible biological inferences that arise from the assumption given by Equations (1) and (2) in Conolly *et al.*, and discuss them in the context of what is known qualitatively. With the assumption in Equation (2), the net growth rate of initiated clones ($\alpha_{\text{I}} - \beta_{\text{I}}$) is made to depend exclusively on the replicative advantage that initiated cells have over normal cells and independent of variations in the death rate of initiated cells. The logic behind Equation (2) was based on the following assumptions. First, for normal cells, $\beta_N(\text{flux}) = \alpha_N(\text{flux})$; that is, the observed cell replication rates are indeed regenerative and to a good approximation balance their death rate. This would be the case on average if, apart from the age-dependent net growth of the normal nasal lining that is specified *a priori* by a growth curve, the total number of normal cells in the lining does not significantly change over time (as required in the model). Second, it was assumed that formaldehyde is equally cytotoxic to initiated and normal cells (since the mechanism is presumed to be via its general chemical reactivity). Then, one obtains $\beta_{\text{I}} = \beta_N = \alpha_N$, in essence bringing the cytotoxic action of formaldehyde to bear strongly upon the parametrization of the CIIT model.

We now examine the implications of juxtaposing the two aspects of the model structure for initiated cells given by Equations (1) and (2) in Conolly *et al.* (2003). The ratio $\alpha_{\text{I}}/\alpha_N$ as a function of formaldehyde flux in Conolly *et al.* (2003) is shown in Fig. 6. For the model specification that best fits the tumor incidence data, $\alpha_{\text{I}}/\alpha_N > 1.0$ for flux $< 27,975$ pmole/mm^2/h, while for higher flux values $\alpha_{\text{I}}/\alpha_N < 1.0$. In Conolly *et al.* while $\beta_{\text{I}} = \alpha_N$ is an assumption, the relationship of $\alpha_{\text{I}} < \alpha_N$ at higher flux is a result of fitting the model to the tumor data. Setting $\beta_{\text{I}} = \alpha_N$ *and* $\alpha_{\text{I}} < \alpha_N$ implies that initiated cells die at a faster rate than they divide, thus reducing the contribution to the calculated tumor probability from elements on the nasal surface that are subject to these higher flux levels. A possible explanation for this effect is that preferential cell-killing

Fig. 6. Flux dependence of ratio of initiated and normal cell replication rates ($\alpha_{\text{I}}/\alpha_N$) in CIIT model. Cell replication rate of initiated cells is less than normal cell replication rate at flux exceeding the value denoted by the arrow. By assumption, the y-axis also represents ($\alpha_{\text{I}}/\beta_{\text{I}}$) in Conolly *et al.* (2003).

due to formaldehyde's cytolethality could lead to extinction of the initiated cell clones in some regions. Second, initiated clones at these flux levels are subject in the model to an extremely high rate of turnover. At these rates, the telomeres of such cells face erosion, eventually leading to extinction of cells (Weinberg, 2007, p. 388). Extinction of initiated clones is also presented in other two-stage modeling endeavors (Luebeck *et al.*, 1991; Kopp-Schneider & Portier, 1992; Bogen, 1998). However, extinction of initiated clones at a specific region of the nasal lining throughout the course of the exposure would effectively prevent the formation of tumors in that region. Therefore, it would be useful to extend the CIIT model to compute site-specific tumor risk and examine its predictions at locations where tumors were observed in the rat. The effect of cytotoxicity on incipient clones of malignantly transformed cells could also be potentially relevant to the location of tumors.

The inference from the model that formaldehyde has a selectively higher cytolethality for initiated cells compared to normal cells at high-enough flux levels is intriguing. Note that the effect of cytolethality on normal cells in Conolly *et al.* (2003) is the observed regenerative increase in cell replication. On the other hand, the inference regarding α_{I} at high flux is obtained on account of the model calibration in Conolly *et al.* and may depend upon the choices made in averaging the cell replication data and in extrapolating those data above the range of observation. Nonetheless, the model structure reconciles these features of tumor-suppression at high formaldehyde fluxes with

its prediction of an overall increase in tumor risk with formaldehyde exposure. In the Appendix, we demonstrate how this is brought about.

There is evidence indicating that generally $\alpha_I > \alpha_N$ in epithelial and other tissue types with or without exposure to specific chemicals (Ceder *et al.,* 2007; Dragan *et al.*, 1995; Schulte-Hermann *et al.*, 1999; Grasl-Kraupp *et al.,* 2000; Coste *et al.*, 1996). With regard to the inference generated by the optimized model in Conolly *et al.* (2003) that $\alpha_I < \alpha_N$ at high flux levels of formaldehyde, it is plausible that the mutation that leads to initiated cells also reduces their responsiveness (and reduces it progressively with greater exposure concentrations) to the general cell replication signals that give rise to increased normal cell replication. There is, however, no direct evidence for verification of this inference.

There are, however, various data that indicate initiated cells to be considerably more resistant to cytotoxicity. Alcohol dehydrogenase 3 (ADH3) is the primary enzymatic defense against formaldehyde. The mRNA levels of ADH3 have been reported to be elevated in the basal layer of human oral epithelial tissue, proliferating cultured human normal oral keratinocytes, and to be dramatically elevated in immortalized human oral keratinocytes compared to normal cells (Hedberg *et al.*, 2000; Nilsson *et al.*, 2004); and, moreover, it has been proposed that ADH3 mRNA is a marker for keratinocyte proliferation (Nilsson *et al.*, 2004). These data suggest that initiated cells may have excess clearance capacity afforded by readily available ADH3 mRNA. Initiated cells in the liver, both spontaneous and chemically induced, have been demonstrated to be resistant to cytotoxicity at an early stage for a large number of chemicals. Such a resistance is manifested variably as decreased ability of the toxicant to induce cell death or to inhibit cell proliferation compared to corresponding effects in normal cells (Farber, 1984; Tsuda *et al.,* 1980). This resistance, thought to be critical to the promotion of liver tumors, is also considered to be brought about by elevated levels of several enzymes, including glutathione transferase isoforms (Glick & Yuspa, 1994).

It is likely that initiated cells already have altered cell cycle control and thus the influence of formaldehyde on apoptosis likely differs between normal and initiated cells. In this regard, *in vitro* models for non-malignant and malignant immortalized human oral keratinocyte cell lines, representing *in vivo* transformed states, exhibit increases in both proliferation and apoptotic rates (Ceder *et al.*, 2007). However,

the immortalized cells are less responsive to signals of terminal differentiation than normal cells (Ceder *et al.,* 2007), and thus this pathway may be impaired in initiated cells *in vivo*. Similarly, p53 mutations are associated with loss of cell cycle control and increased genomic instability (Adimoolam & Ford, 2003), and may represent a marker for initiated cells. Recio *et al.* (1992) identified p53 mutations via PCR in five of eleven formaldehyde-induced tumors in rodent nasal passages. In an expansion of this work, Wolf *et al.* (1995) identified mutant p53 protein in one lesion characterized as preneoplastic, but did not detect such mutants in lesions characterized as nonneoplastic, metaplastic, and hyperplastic. Additionally, higher levels of TGFα were found in preneoplastic cells than in normal cells. Taken together, there are many data to suggest (1) that inferring $\alpha_I < \alpha_N$ at cytotoxic formaldehyde flux levels is problematic, and (2) that β_I would be quite different from β_N.

Thus, in the absence of data to indicate that Equations (1) and (2) are biologically reasonable approaches to link the kinetics of initiated cells with those of normal cells, alternate model structures other than those represented by these relationships considered by Conolly *et al.* need to be explored, given that the two-stage model is extremely sensitive to α_I and β_I. Such an evaluation needs to primarily explore if the assumptions in Equations (1) and (2) significantly impact the intended use of the model, namely, extrapolation to low-dose human cancer risk and the calculation of an upper bound on human risk. Any such alternate model structure needs to provide a good fit to the time-to-tumor data.

As a means of examining an alternate assumption on β_I, there is support to indicate that that some homeostatic mechanisms of growth control are retained in preneoplastic cells so that apoptotic rates and cell replication rates are in general coupled; consequently, death rates of initiated cells would rise with an increase in their division rates (Schulte-Hermann *et al.*, 1997, 1999; Moolgavkar, 1994; Grasl-Kraupp *et al.,* 2000). In the absence of data, other authors (Luebeck *et al.*, 1995; Portier *et al.*, 1996; Luebeck *et al.,* 2000) have assumed the death rate of initiated cells to be proportional to their division rate across dose, that is,
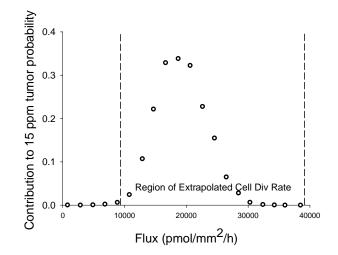
$$\beta_I = \kappa_\beta \cdot \alpha_I,$$

and allowed the constant of proportionality, κ_β, to be estimated by optimization against tumor data.

2.3. Relevance of the Empirical Labeling Index Data and High Flux Bins

As mentioned earlier, the dose response for α_N in Conolly *et al.* (2003) explicitly utilizes the empirical labeling index data for roughly the lower one-fourth (0 to 9,340 pmol/mm^2/h) of the flux range over which the model was calibrated (Fig. 5). To what extent then do the empirical labeling data influence model calibration and results?

In Fig. 7, we plot the probability of tumor at the end of the study versus formaldehyde flux to the rat nasal lining at 15-ppm of formaldehyde exposure concentration. The ordinate is the tumor probability corresponding to the hazard for a given flux bin and is a function of flux at 15-ppm exposure and the number of cells at risk exposed to that flux. (In interpreting this curve, note that it is the hazard, not the probability, that is additive over the flux bins. This is further clarified in the Appendix.) These results have not been reported previously. They were obtained using the source code and data sets kindly provided to us by Dr. Rory Conolly. (It may be noted that the Conolly *et al.* source code we used here is different from the code we developed in our previous article, Subramaniam *et al.* (2007).) We see that the probability of tumor is at the most equal to 0.005 in the flux range from 0 to 9,340 pmol/mm^2/h, while the calibration of the model is most influenced by its fit to the tumor data at 10 and 15 ppm exposure concentrations, largely corresponding to flux greater than 9,340 pmol/mm^2/h. Thus, the replication rates computed directly from the experimentally determined labeling data have limited influence on the fit to the tumor data and, therefore, on the estimation of other model parameters, including those relevant to the low-dose range. On the other hand, we found in our analysis that a 20% increase or decrease in the estimated parameter α_{max} (the cell replication rate corresponding to the upper end of the flux range at 15-ppm exposure) degraded the fit to the tumor incidence data considerably. Because of the interplay between the parameters estimated by optimization, this sensitivity of the model to α_{max} indicates that it is necessary to examine to what extent low-dose estimates of risk are influenced by the uncertainty in its value.

As an aside, we observe from Fig. 7 (and Fig. 1) that the maximum contribution to the probability of tumor at the 15-ppm exposure arises from intermediate levels of formaldehyde flux to the nasal tissue, corresponding to flux bins 8 through 12 in the model.

Fig. 7. Contribution to tumor probability at 15 ppm exposure concentration from 20 flux bins. X-axis is the average flux corresponding to each flux bin. Results correspond to the optimal model in Conolly *et al.* (2003) with the hockey-stick model for cell division rates (their Tables 1 and 4). Dashed lines indicate flux range over which the averaged empirical labeling index data are not available. (See Section 2.1.1.)

This is because the number of cells in the high flux bins is an extremely small fraction in comparison to the total number of cells at risk (as seen from Fig. 2). As exposure concentration decreases, the maximum contribution to the tumor probability comes increasingly from higher flux bin numbers (not shown in the figure but made evident in the Appendix). These results further suggest that the risk of nasal tumor is strongly site-specific across the entire exposure range for reactive gases like formaldehyde. When considered along with the uptake patterns shown in the simulations in Kimbell *et al.* (2001a, 2001b), our results suggest that sites in the rat nose, which present higher risk (for a given exposure), are more anteriorly located at lower exposure than at higher exposures.

The optimal value of α_{max} was found by Conolly *et al.* (2003) to be 0.0435 h^{-1}. As noted by the authors, an argument in support of this value is that it corresponds to the inverse of the fastest cell cycle times found in the literature. Since the model treats the induced replication rates as being time-invariant, it means that cells in the high flux region(s) divide at the highest cell turnover rate ever observed throughout most of an animal's life. Is it possible that such a high level of replication can be sustained? Portions of the anterior rat nose just posterior to the nasal vestibule undergo squamous metaplasia due to sustained formaldehyde exposure, and it is thought

that this transformed cell type is more resistant to formaldehyde-induced toxicity (Kimbell *et al*., 1997). If the induced replication rate is indeed linked tightly with cytotoxicity, this suggests that the highest replication rates are *not* sustained long term.

The need for a sensitivity analysis on the upward extrapolation to α_{max} in Conolly *et al*. (2003) is also indicated by Fig. 3. The value of α_{max} ($\log_{10}\alpha_{max} = -1.37$) in their modeling is roughly an order of magnitude greater than the values of α_N(flux) at the highest flux levels in this figure. If the data pooled over all sites and times are to be used for α_N(flux), then based solely on the trend in α_N(flux) in Fig. 3, it appears unlikely that α_N(flux) could increase up to this value of α_{max}. Visually, these empirically derived data suggest that α_N versus flux may be leveling off rather than increasing ten-fold. Thus, an alternative to the approach taken in Conolly *et al*. (2003) of estimating α_{max} via likelihood optimization against the tumor data is to use regressions of the empirical cell replication data to extrapolate α_N(flux) outside the range of observation (recognizing the uncertainty and model dependence that still results from extrapolating well outside the range of observed data).

2.4. Extrapolating Cell Replication Rates from Rat to Humans

Because there are no equivalent labeling index data available for the human respiratory epithelium, the rat data from Monticello *et al*. (1991, 1996) were also directly applied to estimate cell division rates for humans in Conolly *et al*. (2004). Thus, the curves for the human α_N(flux) or α_I(flux) also acquired the hockey or J-shapes, as considered in the rat model. The only difference in the human estimate was in the fraction of cells considered capable of dividing (81.9% in the rat compared to 66.8% in the humans). As stated by the authors, such an extrapolation assumes that "(1) the labeling indices, both baseline as well as arising from identical exposures to formaldehyde, are the same in rats and humans, and (2) the fractions of cells at risk, that is, having replicative potential, are different."

There are data and arguments to indicate, however, that basal cell division rates differ across species. Considering that enzymatic metabolism plays a role in mitosis, one might expect a lower basal proliferation in humans compared to that in rats. For instance, West and Brown (2005) argue that DNA nucleotide substitution rates scale as mass to the inverse one-fourth power.

But there are other factors that provide a contrary perspective and thereby highlight the scope of uncertainties in the human extrapolation. Chronic exposure to environmental insults is known to affect basal proliferation rates among humans (Calderon-Garciduenas *et al*., 1999), leading to a level of population variability greater than the likely variability among laboratory rats housed in a controlled environment. Calderon-Garciduenas *et al*. found that the replicating fraction of nasal cells (from biopsies) for adult humans living in pristine environments was 14.5%, while for those living in Mexico City ranged from 24–30%. In contrast, Monticello *et al*. (1990) observed labeling indices of 4 and 7% in the septum and lateral meatus, respectively, of control F344 rats. Thus, nominally these observations suggest a higher basal replication rate in humans. Fabrikant and Cherry (1970) observed a labeling index (LI) of 6.1% in normal biopsy tissue from human subjects and also measured the length of the S-phase, thereby estimating a cell doubling time of $\sim$200 hours, which corresponds to a replication rate of $3.5 \cdot 10^{-3}$ h^{-1}.[6] This rate is an order of magnitude greater than the control level ($3 \cdot 10^{-4}$ h^{-1}) used by Conolly *et al*. (2003, 2004). Comparison of these various measures of replication is problematic due to differences in the experimental methods for measuring labeling indices and converting them to replication rates.

Although limited, there are some data that suggest that exposure to formaldehyde increases cell replication at doses far below those that are considered to be cytotoxic. Tyihak *et al*. (2001) treated different human cell lines in culture to various doses (0.1 mM to 10 mM) of formaldehyde and found that the mitotic index increased at the lowest dose of 0.1 mM, a dose that the authors considered to be nontoxic in their experiment. This finding considered along with the episodic nature of human exposure patterns, and human population variability and susceptibility (for example, polymorphisms in ADH3 (Hedberg *et al.*, 2001; Wu *et al.*, 2007)) suggest that human risk estimates in Conolly *et al*. (2004) derived assuming cell replication rates to be higher than baseline levels only under cytotoxic conditions may not be conservative.

An important feature of the human extrapolation in Conolly *et al*. (2004) is that it explicitly

---

[6]We have been unable to find a more recent value in the literature for baseline replication rate (rather than just labeling index) in the human nasal epithelium.

incorporates regional nasal dosimetry of formaldehyde using a finite-element reconstruction of the nasal airways of a single Caucasian adult male (Subramaniam *et al.*, 1998). However, there are considerable interindividual variations in nasal anatomy (ICRP 66, 1994). For example, the nasal volumes of 10 adult nonsmoking subjects between 18 and 50 years of age in a study in the United States varied between 15 ml and 60 ml (Santiago *et al.,* 2001) and disease states can result in further variation (Singh *et al.*, 1998). Therefore, population variability in the regional uptake of formaldehyde could potentially be large. The advantage of the CFD modeling approach, on the other hand, is that it allows for the effect of anatomical variations to be explicitly characterized, and is the subject of currently ongoing work (Garcia *et al.*, 2008.)

Formaldehyde dosimetry is also influenced by the occurrence of squamous metaplasia, an adaptive tissue conversion to squamous that occurs in nasal epithelium exposed to toxic tissue levels of formaldehyde. It has been observed to occur in rats at exposure concentrations of 3 ppm and higher (Kimbell *et al.*, 1997). Squamous epithelium is known to be considerably less absorbing of formaldehyde than other epithelial types (Kimbell *et al.*, 1997). Overall, the highest flux levels of formaldehyde in the simulations in Kimbell *et al.* (2001a) are seen in the region just posterior to the nasal vestibule. A consequence of squamous metaplasia would be to "push" the higher levels of formaldehyde flux toward the more distal regions of the nose (Kimbell *et al.*, 1997). The above dosimetric consequence is, however, not incorporated in the regional flux estimates provided in Kimbell *et al.* (2001a, 2001b) and could be a source of substantial uncertainty in the flux values used in the cancer modeling in Conolly *et al.* (2003). While the metaplastic adaptive effects may not be germane to human exposure scenarios in Conolly *et al.* (2004), they are reflected in the animal labeling index data used in the model. Incorporation of these tissue changes would make the modeling more complex, but the simulations in Kimbell *et al.* (1997) indicate that it would be possible to consider the above effects on dosimetry using their computational approach.

2.5. Use and Estimation of DPX

It was not known whether the DPX directly induced mutations (Conolly *et al.*, 2003; Merk & Speit, 1998); therefore, Conolly *et al.* treated DPX as a dose surrogate indicative of the intercellular concen-

tration of formaldehyde leading to formaldehyde-induced mutations. Regional DPX concentration levels were estimated using a PBPK dosimetry model first developed for the F344 rat and rhesus monkey, and then scaled-up to predict levels in the humans (Conolly *et al.,* 2000). The probability of formaldehyde-induced mutation per cell generation (μ) in the two-stage model was then linearly related to the estimated DPX concentration in the tissue ($\mu = \mu_0 + \text{KMU} \times \text{DPX}$).

The PBPK model in Conolly *et al.* (2000) for predicting DPX levels in humans assumed three first-order rate constants to be the same in humans as in the rat. These rates were for formaldehyde clearance, for formaldehyde binding to DNA, and for DPX repair. Enzymatic metabolism of formaldehyde was assumed to be saturable (in addition to the first-order, nonenzymatic removal rate). The saturation constant K_m was estimated for the rhesus monkey by optimizing against monkey DPX data. For humans, the model used this value of K_m and the epithelial thickness averaged over three regions of the rhesus monkey nose. The maximum rate of metabolism V_{max} was estimated independently for the rat and rhesus monkey by fitting to the DPX data available for these species. This constant was then extrapolated to humans by assuming a power law scaling with body weight (BW); that is, $V_{max} = a \cdot BW^b$, and the coefficient "a" and exponent "b" were derived from the independently estimated values of $(V_{max})_{RAT}$ and $(V_{max})_{RHESUS}$.

The extent of mechanistic data across species, as available in this case, is rarely seen with other chemicals, and the above scale-up procedure was an attempt to use both the rodent and primate DPX data. However, allometric relationships across species are generally based on regressing data from multiple species and usually multiple sources of data points. Thus, the empirical strength of a power-law derived by using two data points (F344 rat and rhesus monkey) is extremely weak for use as an allometric relationship that can then be used to extrapolate to humans. The following observations indicate the need for further understanding of the uncertainty in the values of the parameters V_{max} and K_m in the Conolly *et al.* (2000) models for predicting DPX. First, K_m varies by an order of magnitude across the rat and monkey models but is then considered invariant between the monkey and human models (Conolly *et al.,* 2000). Second, the values in Conolly *et al.* (2000) for V_{max}/K_m, the low-dose limit of the rate of enzymatic metabolism, is roughly

similar between the rat and monkey but lower by a factor of six in humans.

A factor that possibly contributes to these inconsistencies is that a well-mixed compartment is assumed with regard to formaldehyde interaction with DNA and DPX is calculated as the amount of formaldehyde bound to DNA per unit volume of tissue. Formaldehyde and DPX concentrations are likely to have a sharp gradient with distance into the nasal mucosa (Georgieva *et al.*, 2003). Considered together with interspecies differences in tissue thickness, it is therefore uncertain as to whether DPX per unit volume or DPX per unit area of nasal lining is the more appropriate dose metric to be extrapolated.

As mentioned earlier, there are important unresolved questions with regard to the role of DPX in formaldehyde-induced mutagenicity. Studies indicate that DNA lesions remain after DPX removal, resulting in DNA damage (Quievryn & Zhitkovitch, 2000; Speit & Schmid, 2006), and further that the induction of DPX leads to other types of DNA and protein damage (Barker *et al.*, 2005). Cell lines deficient in nucleotide excision repair and DNA-DNA cross-link repair were more sensitive to formaldehyde-induced micronuclei. DPX removal was not different in these cell lines, indicating that events after DPX removal may result in DNA damage (Speit & Schmid, 2006). As such, these findings indicate the potential for formaldehyde-induced mutation after DPX removal and the accumulation of these secondary mutations. Because the residual lesions may be cleared more slowly than DPX (which was modeled as rapidly cleared), treating formaldehyde's mutagenic action as proportional to DPX may underrepresent its mutagenicity. Another potentially significant assumption is that the proportionality constant KMU was considered equal for the first and second mutational event. This assumption was made in order to develop a parsimonious model. Other uncertainties pertaining to DPX clearance and the relevance of rapid hourly variations in DPX levels have been addressed in our previous work (Subramaniam *et al.*, 2007).

3. CONCLUSION

The strength of the CIIT risk assessment for inhaled formaldehyde is its incorporation of mechanistic information at various levels. In particular, it includes important interspecies differences in dosimetry and an amount of quantitative, mechanistic data that are typically not available for a risk as-

sessment (e.g., DPX levels in rats and monkeys). In the case of a highly reactive and soluble gas such as formaldehyde, where portal of entry effects are important, local airway geometry plays a major role in uptake patterns (Kimbell *et al.*, 2001a, 2001b). As there are major differences in rat and human nasal airway geometry and in the number of cells in various sections of the airways, dosimetric differences, which influence site-specific toxicity, may be major determinants of risk. Biologically motivated models that explicitly incorporate such information have the potential to substantially reduce scientific uncertainty in health risk assessment if the impact of model assumptions can be adequately characterized. A novel contribution of the CIIT formaldehyde modeling is that cell replication rates and DNA protein cross-link concentrations are driven by local delivered dose, the formaldehyde flux to each region of nasal tissue, predicted for anatomically accurate representations of the nasal passages.

Analysis of the CIIT effort helps identify a range of biological and statistical issues that can arise in the use of biologically-based dose-response models for low-dose extrapolation of cancer risk. The uncertainties we identify in this article are both qualitative and quantitative in nature and arise in the use of the available cell replication, tumor, and DPX data, in the model specification, and in the evaluation of parameters. These issues, examined in the context of modeling the data on F344 rats in Conolly *et al.* (2003), mainly pertain to:

1. the model structure for initiated cells in the context of no data and the extreme sensitivity of a two-stage model to initiated cell birth and death rates;
2. the characterization of the dose-response curve for normal cell replication rates, including the upward extrapolation of this curve over a major part of the tissue dose range over which the model is parameterized;
3. the appropriateness of combining pulse and continuous labeled data as a time-weighted average over all sites; and
4. the potential importance of reflecting the variability in normal cell replication rates across nasal sites

In addition, we identified a limited set of issues in Conolly *et al.* (2004) that we believe to impact the scale-up of risk estimates from rats to humans the most. The CIIT effort faces the difficulty that is

common to most interspecies extrapolation of toxicologic data: the lack of human data for estimation of necessary parameters and variability in humans. This difficulty also exists when default extrapolation methods are used, but the mechanistic details in a biologically motivated model can make the lack of human data and the resulting uncertainties explicit and identifiable. On the other hand, a biologically motivated model, such as the CIIT model, where the extent of assumptions and uncertainties is large, can result in replacing general relationships in a baseline scientific explanation having some empirical support with much more specific assumptions. These latter assumptions can have a large impact on risk extrapolation and, although appearing scientifically plausible, may have limited empirical support. In using the human extrapolation in Conolly *et al.* (2004), we mainly identified uncertainties in:

1. extrapolating rodent tumor formation to humans as parameterized in this model by the use of rodent cell labeling data;
2. estimation of mutation dose response, which is assumed to depend here on the internal dose metric of DPX concentrations.

Conolly *et al.* (2004) characterized the *deminimis* human risk estimates derived from this model as being "conservative in face of model uncertainties." This assessment of conservatism was based, in part, upon their (1) use of the "hockey-stick" dose response for cell replication rates when the time-weighted average of cell replication rates over sites allowed a J-shaped curve in the F344 rat; (2) inclusion of overall respiratory cancer incidence in estimation of baseline parameters in the human model; and (3) use of an upper bound for the coefficient relating formaldehyde-induced mutation to DPX concentrations. Given the potentially significant uncertainties identified in this article and in the limited analyses presented in Subramaniam *et al.* (2007), we believe that such a characterization is premature. A documented evaluation of these uncertainties and, in the absence of data, the examination of alternate model structures is therefore needed. The characterization of initiated cell kinetics in the modeling is particularly debatable in view of the extreme sensitivity of two-stage model risk estimates on initiated cell replication and death rates. Because of the paucity of these data, in this article we probed the inferences arising from the CIIT model structure for support from related biological evidence. The arguments presented in this article provide grounds for considering the CIIT model structure as plausible. However, the biological evidence also provide strong motivation to consider very different relationships between the initiated and normal cells with regard to their replication and death rates than that considered in Conolly *et al.* (2003, 2004). This is likely to be the most important of uncertainties that can substantially impact both the rat clonal growth model for formaldehyde-induced nasal cancer as well as the corresponding model for extrapolation to the human respiratory tract.

ACKNOWLEDGMENTS

APPENDIX

Here we examine further our inference that exposure to certain levels of regional formaldehyde flux leads to extinction of initiated cell clones (i.e., $\beta_I(\text{flux}) > \alpha_I(\text{flux})$) in the Conolly *et al.* (2003)
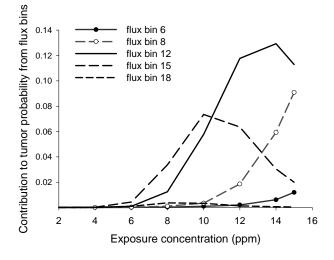
model. How is this reconciled with the fact that the overall tumor data to which the model is fitted are monotonic with exposure concentration (ppm)? We probe this by examining model predictions for different flux bins at various exposure concentrations. In the model structure in Conolly *et al.* (2003), the overall hazard at a given exposure concentration is decomposed additively in terms of solutions for each flux bin. Then, if $P_i(T)$ is the contribution to the tumor probability due to the average formaldehyde flux from flux bin "i" at a given exposure concentration, the cumulative probability of tumor at time T for the overall nose can be written as

$$P(T) = 1 - \prod_i [1 - P_i(T)],$$

where the product is over the 20 flux bins. $P_i(T)$ is a function of formaldehyde flux delivered to cells in bin "i" and the number of cells at risk in that bin. Recall now that:

1. the average flux corresponding to a given flux bin increases linearly with exposure concentration, and is given by Fig. 1, and
2. the spatial coordinates of the elements of the nasal lining corresponding to a flux bin (that is, receiving a given interval of flux per ppm of exposure concentration) are fixed in location as exposure concentration changes in the model.[7] Therefore, a pertinent question is how $P_i(T)$ changes with exposure concentration.

Fig. A1 shows $P_i(T)$ for five flux bins ($i = 6$, 8, 12, 15, 18) as a function of exposure concentration for $T = 793$ days.[8] The results correspond to the optimal model in Conolly *et al.* (2003) using parameters from Table 4 and using the hockey-stick-shaped cell replication rates from Table 1 of that article. The results show a rapid decrease in the contribution to the tumor probability from flux bins 15 and 18 for exposure concentrations greater than 10 ppm and 8 ppm, respectively. For flux bin 12, P_i decreases only for exposure concentrations greater than 14 ppm. On the other hand, P_i corresponding to bins 6 and 8 are monotonically increasing with ex-

---

[7]Note that these elements may generally be discontiguous across the nasal surface.

[8]Note that the 15 ppm exposure data in Conolly *et al.* (2003) is for a longer duration. However, the purpose in Fig. A1 is to examine model behavior as a function of exposure. Therefore, T was maintained the same for all exposure concentrations in these simulations.

Fig. A1.

posure. Thus, in essence, the drop in P_i that is seen for some flux bins is "compensated" by the monotonically increasing P_i for the other flux bins, and allows for the overall tumor probability for the entire nose to be monotonically increasing with exposure concentration. (Note that this figure is specific to the 20-bin structure of the CIIT model. If the number of bins changes, the average flux corresponding to each bin also changes.) These results have not been reported previously.

Is the nonmonotonic nature of some curves in Fig. A1 plausibly an expression of cell killing at cytotoxic levels of local flux? It will be useful to examine whether alternate biologically plausible model structures for initiated cells also result in such a prediction.

REFERENCES

Adimoolam, S., & Ford, J. M. (2003). p53 and regulation of DNA damage recognition during nucleotide excision repair. *DNA Repair*, 2, 947–954.

Barker, S., Weinfeld, M., & Murray, D. (2005). DNA-protein crosslinks: Their induction, repair, and biological consequences. *Mutation Research*, 589, 111–135.

BfR. (2006). *Toxicological Assessment of Formaldehyde*. Opinion of BfR No. 023/2006. Available at http://www.bfr.bund.de/cm/290/toxicological_assessment_of_formaldehyde.pdf.

Bogen, K. T. (1998). Mechanistic model predicts a U-shaped relation of radon exposure to lung cancer risk reflected in combined occupational and U.S. residential data. *Human & Experimental Toxicology*, 17, 691–696.

Bull, R. J. (2000). Mode of action of liver tumor induction by trichloroethylene and its metabolites, trichloroacetate and dichloroacetate. *Environmental Health Perspectives*, 108(Suppl 2), 241–259.

Calderon-Garciduenas, L., Rodriguez-Alcaraz, A., Garcia, R., Barragan, G., Villarreal-Calderon, A., & Madden, M. C.

(1999). Cell proliferation in nasal respiratory epithelium of people exposed to urban pollution. *Carcinogenesis*, 20, 383–389.

CalEPA. (2005). Letter from JR Froines, Chair of Scientific Review Panel to B Jordan, Interim Chairperson, Air Resources Board, California Environment Protection Agency.

Ceder R., Merne, M., Staab C., Nilsson, J. A., Hoog, J. O., Dressler, D., Engelhart, K., & Grafstrom, R. C. (2007). The application of normal, SV40 T-antigen-immortalised and tumour-derived oral keratinocytes, under serum-free conditions, to the study of the probability of cancer progression as a result of environmental exposure to chemicals. *Alternatives to Laboratory Animal*, 35, 621–639.

CIIT. (1999). Formaldehyde: Hazard characterization and dose-response assessment for carcinogenicity by route of inhalation. Report, Chemical Industry Institute of Toxicology, Research Triangle Park, North Carolina.

Conolly, R. B., Kimbell, J. S., Janszen, D. B., & Miller, F. J. (2002). Dose response for formaldehyde-induced cytotoxicity in the human respiratory tract. *Regulatory Toxicology Pharmacology*, 35, 32–43.

Conolly, R., Kimbell, J., Janszen, D., Schlosser, P., Kalisak, D., & Preston, J. (2003). Biologically motivated computational modeling of formaldehyde carcinogenicity in the F344 rat. *Toxicological Sciences*, 75, 432–447.

Conolly, R., Kimbell, J., Janszen, D., Schlosser, P., Kalisak, D., Preston, J. *et al.* (2004). Human respiratory tract cancer risks of inhaled formaldehyde: Dose-response predictions derived from biologically-motivated computational modeling of a combined rodent and human dataset. *Toxicological Sciences*, 82, 279–296.

Conolly, R., Lilly, P., & Kimbell, J. (2000). Simulation modeling of the tissue disposition of formaldehyde to predict nasal DNA-protein cross-links in Fischer 344 rats, rhesus monkeys, and humans. *Environmental Health Perspectives*, 108, 919–924.

Conolly, R. B., & Lutz, W. K. (2004). Nonmonotonic dose-response relationships: Mechanistic basis, kinetic modeling, and implications for risk assessment. *Toxicological Sciences*, 77, 151–157.

Coste A., Rateau, J. G., Roudot-Thoraval, F., Chapelin, C., Gilain, L., Poron F., Peynegre, R., & Bernaudin, J. F., Escudier, E. (1996). Increased epithelial cell proliferation in nasal polyps. *Archives of Otolaryngology Head & Neck Surgery*, 122(4), 432–436.

Dragan, Y. P., Hully, J., Baker, K., Crow, R., Mass, M. J., & Pitot, H. C. (1995). Comparison of experimental and theoretical parameters of the Moolgavkar-Venzon-Knudson incidence function for the stages of initiation and promotion in rat hepatocarcinogenesis. *Toxicology*, 102, 161–175.

Fabrikant, J. I., & Cherry, J. (1970). The kinetics of cellular proliferation in normal and malignant tissues. X. Cell proliferation in the nose and adjoining cavities. *Annals Otology Rhinology Laryngology*, 79, 572–578.

Farber E. (1984). Cellular biochemistry of the stepwise development of cancer with chemicals: G. H. A. Clowes memorial lecture. *Cancer Research*, 44(12), 5463–5474.

Garcia, G. J. M., Schroeter, J. D., Segal, R. A., Stanek, J., Foureman, G. L., & Kimbell, J. S. (2008). Dosimetry of nasal uptake of soluble and reactive gases: A first study of inter-human variability. *Inhalation Toxicology*, in press.

Gaylor, D. W., Lutz, W. K., & Conolly, R. B. (2004). Statistical analysis of nonmonotonic dose-response relationships: Research design and analysis of nasal cell proliferation in rats exposed to formaldehyde. *Toxicological Sciences*, 77, 158–164.

Georgieva, A. V., Kimbell, J. S., & Schlosser, P. M. (2003). A distributed-parameter model for formaldehyde uptake and disposition in the rat nasal lining. *Inhalation Toxicology*, 15, 1435–1463.

Glick A., & Yuspa, S. H. (1994). Tumor promotion and carcinogenesis. In P. E. Angel & P Herrlich (Eds.), *The Fos and Jun Families of Transcription Factors* (Chapter 19). Boca Raton, FL: CRC Press.

Grasl-Kraupp, B., Luebeck, G., Wagner, A., Low-Baselli, A., de, G. M., Waldhor, T. *et al.* (2000). Quantitative analysis of tumor initiation in rat liver: Role of cell replication and cell death (apoptosis). *Carcinogenesis*, 21, 1411–1421.

Health Canada. (2001). *Priority Substances List Assessment Report: Formaldehyde*. ISBN 0-662-29447-5. Cat. no. En40-215/61E.

Heck, H., & Casanova, M. (1999). Pharmacodynamics of formaldehyde: Applications of a model for the arrest of DNA replication by DNA-protein cross-links. *Toxicology & Applied Pharmacology*, 160, 86–100.

Hedberg, J. J., Backlund, M., Stromberg, P., Lonn, S., Dahl, M. L., Ingelman-Sundberg, M., & Hoog, J. O. (2001). Functional Polymorphism in the alcohol dehydrogenase 3 (ADH3) promoter. *Pharmacogenetics*, 11, 815–824.

Hedberg, J. J., Hoog, J. O., Nilsson, J. A., Xi, Z., Elfwing, A., & Grafstrom, R. C. (2000). Expression of alcohol dehydrogenase 3 in tissue and cultured cells from human oral mucosa. *American Journal of Pathology*, 157, 1745–1755.

ICRP 66. (1994). Human respiratory tract model for radiological protection. *Annals of the ICRP*, 24, 36.

Kerns, W., Pavkov, K., Donofrio, D., Grlla, E., & Swenberg, J. (1983). Carcinogenicity of formaldehyde in rats and mice after long-term inhalation exposure. *Cancer Research*, 43, 4382–4392.

Kimbell J. S., Gross E.A., Richardson R. B., Conolly R. B., & Morgan K. T. (1997). Correlation of regional formaldehyde flux predictions with the distribution of formaldehyde-induced squamous metaplasia in F344 rat nasal passages. *Mutation Research*, 380, 143–154.

Kimbell, J., Overton, J., Subramaniam, R., Schlosser, P., Morgan, K., & Conolly, R. (2001a). Dosimetry modeling of inhaled formaldehyde: Binning nasal flux predictions for quantitative risk assessment. *Toxicological Sciences*, 64, 111–121.

Kimbell, J., Subramaniam, R., Gross, E., Schlosser, P., & Morgan, K. (2001b). Dosimetry modeling of inhaled formaldehyde: Comparisons of local flux predictions in the rat, monkey, and human nasal passages. *Toxicological Sciences*, 64, 100–110.

Kopp-Schneider, A., & Portier, C. J. (1992) Birth and death/differentiation rates of papillomas in mouse skin. *Carcinogenesis*, 13, 973–978.

Liteplo, R. G., & Meek, M. E. (2003). Inhaled formaldehyde: Exposure estimation, hazard characterization, and exposure-response analysis. *Journal of Toxicology Environmental Health B Critical Reviews*, 6, 85–114.

Luebeck, E. G., Buchmann, A., Stinchcombe, S., Moolgavkar, S. H. & Schwarz, M. (2000). Effects of 2,3,7,8-tetrachlorodibenzo-p-dioxin on initiation and promotion of GST-P-positive foci in rat liver: A quantitative analysis of experimental data using a stochastic model. *Toxicology & Applied Pharmacology*, 167, 63–73.

Luebeck, E. G., Grasl-Kraupp, B., Timmermann-Trosiener, I., Bursch, W., Schulte-Hermann, R., & Moolgavkar, S. H. (1995). Growth kinetics of enzyme-altered liver foci in rats treated with phenobarbital or alpha-hexachlorocyclohexane. *Toxicology & Applied Pharmacology*, 130, 304–315.

Luebeck, E. G., Moolgavkar S. H., Buchmann A., & Schwarz, M. (1991). Effects of polychlorinated biphenyls in rat liver: Quantitative analysis of enzyme-altered foci. *Toxicology Applied Pharmacology*, 111(3), 469–484.

MAK Commission. [German Commission for the Investigation of Health Hazards of Chemical Compounds in the Work Area]. (2006). Formaldehyde, Official English Translation, Occupational Toxicants: Critical Data Evaluation for MAK values and Classification of Carcinogens, Vol. 17, 163.

Merk, O., & Speit, G. (1998). Significance of formaldehyde-induced DNA-protein crosslinks for mutagenesis. *Environmental & Molecular Mutagenesis*, *32*, 260–268.

Monticello, T., Miller, F., & Morgan, K. (1991). Regional increases in rat nasal epithelial cell proliferation following acute and subchronic inhalation of formaldehyde. *Toxicology & Applied Pharmacology*, *111*, 409–421.

Monticello, T. M., Morgan, K. T., & Hurtt, M. E. (1990). Unit length as the denominator for quantitation of cell proliferation in nasal epithelia. *Toxicologic Pathology*, *18*, 24–31.

Monticello, T., Swenberg, J., Gross, E., Leininger, J., Kimbell, J., Seilkop, S., Starr, T. B., Gibson, J. E., & Morgan, K. T. (1996). Correlation of regional and nonlinear formaldehyde-induced nasal cancer with proliferating populations of cells. *Cancer Research*, *56*, 1012–1022.

Moolgavkar, S. H. (1994). Biological models of carcinogenesis and quantitative cancer risk assessment. *Risk Analysis*, *14*, 879–882.

Moolgavkar, S., Dewanji, A., & Venzon, D. (1988). A stochastic two-stage model for cancer risk assessment. I. the hazard function and the probability of tumor. *Risk Analysis*, *8*, 383–392.

Moolgavkar, S. H., & Luebeck, E. G. (1990). Two-event model for carcinogenesis: Biological, mathematical, and statistical considerations. *Risk Analysis*, *10*, 323–341.

Moolgavkar, S. H., & Luebeck, E. G. (1992). Interpretation of labeling indices in the presence of cell death. *Carcinogenesis*, *13*, 1007–1010.

Morgan, K. T. (1997). A brief review of formaldehyde carcinogenesis in relation to rat nasal pathology and human health risk assessment. *Toxicologic Pathology*, *25*, 291–307.

Nilsson, J. A., Hedberg, J. J., Vondracek, M., Staab, C. A., Hansson, A., Hoog, J. O., & Grafstrom, R. C. (2004). Alcohol dehydrogenase 3 transcription associates with proliferation of human oral keratinocytes. *Cellular and Molecular Life Sciences*, *61*, 610–617.

Overton, J. H., Kimbell, J. S., & Miller, F. J. (2001). Dosimetry modeling of inhaled formaldehyde: The human respiratory tract. *Toxicological Sciences*, *64*, 122–134.

Portier C. J., Sherman C. D., Kohn M., Edler L., Kopp-Schneider A., Maronpot R. M., & Lucier G. (1996). Modeling the number and size of hepatic focal lesions following exposure to 2,3,7,8-TCDD. *Toxicology & Applied Pharmacology*, *138*(1), 20–30.

Quievryn, G., & Zhitkovitch, A. (2000). Loss of DNA-protein crosslinks from formaldehyde-exposed cells occurs through spontaneous hydrolysis and an active repair process linked to proteosome function. *Carcinogenesis*, *21*, 1573–1580.

Recio, L. (1997). Oncogene and tumor suppressor gene alterations in nasal tumors. *Mutation Research*, *380*, 27–31.

Recio, L., Sisk, S., Pluta, L., Bermudez, E., Gross, E. A., Chen, Z., Morgan, K., & Walker, C. (1992). p53 mutations in formaldehyde-induced nasal squamous cell carcinomas in rats. *Cancer Research*, *52*, 6113–6116.

Rotstein, J., Sarma, D. S. R., & Farber, E. (1986). Sequential alterations in growth control and cell dynamics of rat hepatocytes in early precancerous steps in hepatocarcinogenesis. *Cancer Research*, *46*, 2377–2385.

Santiago, L. Y., Hann, M. C., Ben-Jebria, A., & Ultman, J. S. (2001). Ozone absorption in the human nose during unidirectional airflow. *Journal of Applied Physiology*, *91*, 725–732.

Schulte-Hermann, R., Bursch, W., Grasl-Kraupp, B., Marian, B., Torok, L., Kahl-Rainer, P. *et al.* (1997). Concepts of cell death

and application to carcinogenesis. *Toxicologic Pathology*, *25*, 89–93.

Schulte-Hermann, R., Bursch, W., Marian, B., & Grasl-Kraupp, B. (1999). Active cell death (apoptosis) and cellular proliferation as indicators of exposure to carcinogens. *IARC Science Publication*, 273–285.

Shaham, J., Bomstein, Y., Gurvich, R., Rashkovsky, M., & Kaufman, Z. (2003). DNA-protein crosslinks and p53 protein expression in relation to occupational exposure to formaldehyde. *Occupational Environmental Medicine*, *60*(6), 403–409.

Singh, G. D., McNamara, J. A. Jr., & Lozanoff, S. (1998). Morphometry of the midfacial complex in subjects with class III malocclusions: Procrustes, Euclidean, and cephalometric analyses. *Clinical Anatomy*. *11*, 162–170.

Snedecor, G. W., & Cochran, W. G. (1980). *Statistical Methods*, 7th ed. Ames, IA: Iowa State University Press.

Speit, G., & Schmid, O. (2006). Local genotoxic effects of formaldehyde in humans measured by the micronucleus test with exfoliated epithelial cells. *Mutation Research*, *613*, 1–9.

Subramaniam, R. P., Crump K. S., Van Landingham C., White, P., Chen, C., & Schlosser, P. M. (2007). Uncertainties in the CIIT model for formaldehyde-induced carcinogenicity in the rat: A limited sensitivity analysis-I. *Risk Analysis*, *27*(5), 1237–1254.

Subramaniam, R. P., Richardson, R. B., Morgan, K. T., Kimbell, J. S., & Guilmette, R. A. (1998). Computational fluid dynamics simulations of inspiratory airflow in the human nose and nasopharynx. *Inhalation Toxicology*, *10*, 91–120.

Tsuda, H., Lee, G., & Farber, E. (1980). Induction of resistant hepatocytes as a new principle for a possible short-term in vivo test for carcinogens. *Cancer Research*, *40*(4), 1157–1164.

Tyihak, E., Bocsi, J., Timar, F., Racz, G., & Szende, B. (2001). Formaldehyde promotes and inhibits the proliferation of cultured tumour and endothelial cells. *Cell Proliferation*, *34*(3), 135–141.

USEPA. (2006a). *Health Effects Information Used in Cancer and Noncancer Risk Characterization for the 1999 National-Scale Assessment (NATA)*. Available at http://www.epa.gov/ttn/atw/nata1999/99pdfs/healtheffectsinfo.pdf.

USEPA. (2006b). National emission standards for hazardous air pollutants: Plywood and composite wood products; List of hazardous air pollutants, lesser quantity designations, source category list; Final rule. 40 CFR 63. *Federal Register*, *71*(32), 8341–8387.

Weinberg, R. A. (2007). *The Biology of Cancer*. New York: Garland Science.

West, G. B., & Brown, J. H. (2005). The origin of allometric scaling laws in biology from genomes to ecosystems: Towards a quantitative unifying theory of biological structure and organization. *Journal of Experimental Biology*, *208*, 1575–1592.

Wolf, D. C., Gross, E. A., Lyght, O., Bermudez, E., Recio, L., & Morgan, K. T. (1995). Immunohistochemical localization of P53, PCNA and TGF-a proteins in formaldehyde-induced rat nasal squamous cell carcinomas. *Toxicology & Applied Pharmacology*, *132*, 27–35.

Wu, H., Romieu, I., Sienra-Monge, J. J., Estela Del Rio-Navarro, B., Anderson, D. M., Jenchura, C. A., Li, H., Ramirez-Aguilar, M., Del Carmen Lara-Sanchez, I., & London, S. J. (2007). Genetic variation in S-nitrosoglutathione reductase (GSNOR) and childhood asthma. *Journal of Allergy and Clinical Immunology*, *120*, 322–328.